Water Supply

IWA PUBLISHING

Water Supply Vol 22 No 3, 3553 doi: 10.2166/ws.2021.384

Experimental study of the effect of nanoscale zero-valent iron injected on the permeability of saturated porous media

Jie Tang[a,b], Fei Liu[a,b,*], Chong Zhang[a,b] and Qiang Xue[a,b]

[a] MOE Key Laboratory of Groundwater Circulation and Environmental Evolution, China University of Geosciences (Beijing), Beijing 100083, PR China
[b] Beijing Key Laboratory of Water Resources and Environmental Engineering, School of Water Resources and Environment, China University of Geosciences, Beijing 100083, PR China
*Corresponding author. E-mail: feiliu@cugb.edu.cn

ABSTRACT

In a comparison of modified nanoscale zero-valent iron (NZVI), bare NZVI used to remediate deep contaminated groundwater source areas has more advantages. However, the influence of injected bare NZVI deposition on the permeability of aquifer remains unclear, together with which are still the key factors of engineering cost and contamination removal. Hence, this study sought to assess a method of measuring hydraulic conductivity with a constant head device and to examine the permeability loss mechanism of NZVI injected into different saturated porous media, using column tests. The results showed that it was feasible to determine hydraulic conductivity by the constant head device. The permeability loss caused by NZVI injection increased with a decrease in the grain size of the porous media, and was determined by the amount and distribution of NZVI deposition. The NZVI distribution area had a good linear correlation with dispersivity of the porous media. Additionally, although surface clogging occurred in all porous media, the amount of NZVI deposition at the injection point was largest in fine sand, so that its permeability loss was the most; this was more likely to cause hydraulic fracturing and expand the area of the contaminant source zone. These results have implications for NZVI field injection for successful groundwater remediation.

Key words: clogging, deposition, dispersivity, nanoscale zero-valent iron, permeability loss, saturated porous media

HIGHLIGHTS

- The amount and distribution of NZVI deposition determines permeability loss.
- NZVI distribution area has a good positive linear correlation with dispersivity of the porous media.
- Coarse and medium sand were classified as mix clogging, while fine sand was surface clogging.

GRAPHICAL ABSTRACT

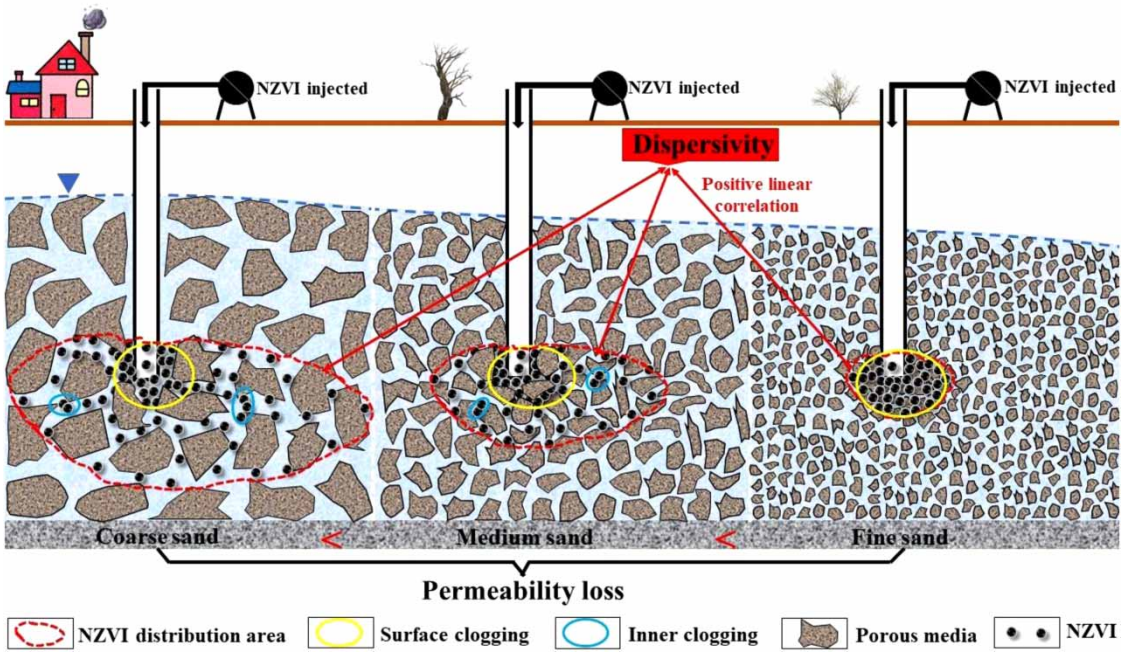

1. INTRODUCTION

Over the last two decades, nanoscale zero-valent iron (NZVI) with a typical core–shell structure has received significant attention as a promising material for the in-situ remediation of contaminated groundwater (Wei *et al.* 2010; Fu *et al.* 2014; Tosco *et al.* 2014). NZVI can be used to treat a wide range of contaminants through adsorption, reduction, oxidation and precipitation, of which reduction is the main function (Zou *et al.* 2016; Wu *et al.* 2017; Yang *et al.* 2019; Yang *et al.* 2021). Compared with granular zero-valent iron (ZVI), the main advantages of NZVI are stronger reactivity due to its high specific surface area (SSA) and flexible injection into contaminated aquifer due to its small size, especially for the aquifer with a depth of more than 40 m (Karn *et al.* 2009; Comba *et al.* 2011; Guan *et al.* 2015; Mondal *et al.* 2021). However, the critical issues faced by the application of NZVI in porous media are weak migration performance and significant loss of permeability, which were observed at both indoor experiments and field applications (Zheng *et al.* 2008; Noubactep *et al.* 2012).

In order to overcome these shortcomings, much effort has been made to modify or stabilize NZVI by using polyelectrolytes, polymers and surfactants [such as carboxymethyl cellulose (CMC) and polyacrylic acid (PAA)] (He *et al.* 2009; Strutz *et al.* 2016a; Micic *et al.* 2020), or directly modify the NZVI surface during synthesis by adding noble metals [such as copper (Cu) and nickel (Ni)] (Harendra & Vipulanandan 2011; Hosseini & Tosco 2013; He *et al.* 2018). The role of surface modification is mainly to improve the migration performance of NZVI applying the following three points: (1) Reduce the Fe^0 content, which indirectly reduces the magnetic attraction between nanoparticles. (2) Introduce static electricity or steric repulsion between nanoparticles to prevent the formation of large agglomerates. (3) Increase the repulsive force between nanoparticles and porous media (Tosco *et al.* 2014). To this end, several column tests have been reported in the literature aimed to investigate the migration performance of surface modified or stabilized NZVI using particle breakthrough curves in one- or two- dimensional saturated porous media, under different types and concentrations of modifier (Phenrat *et al.* 2010; Raychoudhury *et al.* 2010, 2014), properties of porous media (Jung *et al.* 2014; Strutz *et al.* 2016b; Mystrioti *et al.* 2020), hydrochemical characteristics (Saleh *et al.* 2008; Dong & Lo 2013; Micic *et al.* 2020) and hydrodynamic conditions (Hosseini & Tosco 2013; Strutz *et al.* 2016a; Ostad-Ali-Askari & Shayannejad 2021). To reveal the migration and deposition mechanism of surface modified NZVI in porous media, a series of numerical models of migration and deposition was created to describe and evaluate their behavior (Phenrat *et al.* 2009a; Tian *et al.* 2010; Hosseini & Tosco 2013; Babakhani *et al.* 2018).

The deposition of NZVI during the migration process could cause clogging of porous media, which would lead to a decrease in porosity and permeability, and ultimately affect the remediation effect of NZVI on contaminated groundwater.

Based on the physicochemical deposition and release mechanism of NZVI amended with xanthan gum in porous media, an expression between the porosity and permeability of aquifer and NZVI deposited on the surface of porous media was established, and was used to simulate clogging of porous media caused by the deposition of nanoparticles (Tosco & Sethi 2010). The deposition of NZVI during the migration process is affected by the nature of porous media and NZVI, and flow velocity (Mondal *et al.* 2021). Strutz *et al.* (2016b) injected PAA-NZVI into horizontal porous media sand columns filled with different particle sizes, and observed that the deposition of NZVI increased and the permeability decreased faster in sand columns with smaller particle sizes, thus quantifying the effects of particle size and NZVI deposition on porosity and permeability of porous media. Subsequently, they also discussed the effect of injection flow velocity and injection concentration on the spatial distribution and deposition process of NZVI in porous media, and quantified the decrease in permeability of porous media due to NZVI deposition through experimental tests and numerical simulations (Strutz *et al.* 2016a). Additionally, Hosseini & Tosco (2013) reported that Fe/Cu nanoparticle injection could result in pore clogging due to deposition, which could be observed by pressure drops, especially at concentration of 8 and 12 g/L. Simultaneously, they also showed that a higher injection velocity is more conducive to NZVI deposited in porous media, which would led to more clogging.

Reduce in permeability of the aquifer may cause groundwater bypass and not be conducive to NZVI technology to remediate contaminated plumes of groundwater. Modified NZVI has been extensively reported to enhance the migration ability and then reduce permeability loss in previous studies. However, reduced permeability is not always a disadvantage, especially for treatment of contaminant source zones. It can trap the release of contamination and play a key role in reducing flux decided by NZVI reactivity. The NZVI used for remediation of contaminated sources of deep groundwater areas only needs to be kept at the target source area (Strutz *et al.* 2016b) and to provide more electronics, which makes bare NZVI more advantageous as modified NZVI greatly reduced the Fe^0 content and reactivity (Phenrat *et al.* 2009b; Tosco *et al.* 2014). Currently, the influences of injected bare NZVI deposition on the permeability of aquifers remain unclear, such as permeability loss and distribution area of NZVI deposition, which are still the key factors in engineering cost and contamination removal. In this study, NANOFER STAR provided by NanoIron s.r.o. (Czech Republic) was selected as the research object. The primary objective was to evaluate the permeability of porous media decided with the constant head device, and to investigate the deposition law of NZVI and permeability loss in different saturated porous media after injection using by column experiments. This research provides an important theoretical basis for NZVI injection to successfully remediate contaminated groundwater.

2. MATERIALS AND METHODS

If not specified, all the chemicals used in this study were of analytical grade and purchased from Beijing Chemical Corp., China. All solutions were prepared using deoxygenated ultrapure water (Millipore Corp, USA).

2.1. Characterization of NZVI

NZVI provided by NanoIron s.r.o. (Czech Republic) is an air-stable nZVI powder, named as NANOFER STAR. NZVI is in the form of clusters and agglomerates, so passes through a 75 μm sieve for experimental use. Analysis by X-ray diffraction (XRD) (Bruker D8 Advance, Germany) with Cu Kα radiation at 40 kV/250 mA, NZVI consisted of α-Fe (characteristic XRD peak at 44.6°) and magnetite as described in Supplementary Material, Figure S1. According to the manufacturer, NZVI had a typical spherical core–shell structure, and the mean particle size of NZVI was 59.8 nm and oxide layer thickness was 4.3 nm as shown in Supplementary Material, Figure S2.

2.2. Properties of porous media

Here, 0.1–0.85 mm (20–140 mesh) quartz sand purchased from Sinopharm Chemical Reagent Beijing Co., Ltd were divided into coarse sand (0.5–0.85 mm), medium sand (0.3–0.5 mm) and fine sand (0.1–0.3 mm), and used as the quartz porous media. Some metal oxide and organic impurities on the quartz sand may have influenced nZVI migration and resulted in deposition at its surface (Litton & Olson 1993). Therefore, the sand was washed with ultrapure water, hydrogen peroxide and hydrochloric acid (HCl), following the procedure described by Mystrioti *et al.* (2015). The basic properties of quartz sand are shown in Table 1. The dry density of quartz sand was calculated based on its mass and volume, which were determined using the Archimedes' overflow method. The SSA measurement of quartz sand was made by physical adsorption equipment (ASAP 2460, USA), based on the Brunauer, Emmett and Teller (BET) method of N_2 adsorption. Mastersizer

Table 1 | The basic properties of quartz sand

Quartz sand type	Grain size mm	Dry density g/cm^3	Mechanical composition						SSA m^2/kg
			d_{10} mm	d_{30}	d_{50}	d_{60}	C_u	C_c	
Coarse sand	>0.5	2.51	0.42	0.56	0.64	0.68	1.62	1.08	74.9 ± 1.5
Medium sand	0.3–0.5	2.56	0.21	0.32	0.40	0.44	2.10	1.11	93.1 ± 0.8
Fine sand	<0.3	2.69	0.11	0.19	0.24	0.28	2.57	1.15	110.9 ± 1.6

Note: d_{10}, d_{30}, d_{50} and d_{60} are grain sizes of the cumulative mass of quartz sand accounting for 10, 30, 50 and 60% of the total mass, respectively; C_u and C_C are calculated by d_{60}/d_{10} and $(d_{30})^2/(d_{10}d_{60})$, respectively.

2000 (UK) was used to analyze the mechanical composition of quart sand. Additionally, the porous media used in the experiment had good uniformity and sorting, as shown in Supplementary Material, Figure S3.

2.3. Experimental methods

The column experiments were conducted using three types quartz sand column. Figure 1 is composed of two parts showing the schematic of column setup. Among them, Figure 1(a) describes the experimental column saturation, bromide ion (Br^-) penetration, NZVI injection and flushing process, and Figure 1(b) determines permeability of saturated porous media before and after NZVI injection. The hydraulic conductivity of sand column was calculated by the Darcy equation, as follows:

$$V = \frac{Q}{A} = KI = K\frac{\Delta H}{L} \tag{1}$$

where V is Darcy flow velocity, m/d; Q is outlet flow, m^3/d; A is the cross-sectional area of sand column, m^2; K is the hydraulic conductivity of sand column; I is hydraulic gradient; ΔH is head difference, cm; L is length of sand column, cm.

(1) Packed columns and measured pore size

The columns were constructed using organic glass pipe (10 cm in height and 2 cm in inner diameter). The coarse, medium and fine sand was packed into each column using the dry method (each weighing 2.3 g and the filling height ~0.5 cm, repeated), respectively. Before the column was encapsulated, the quartz sand loaded in the column was consolidated by

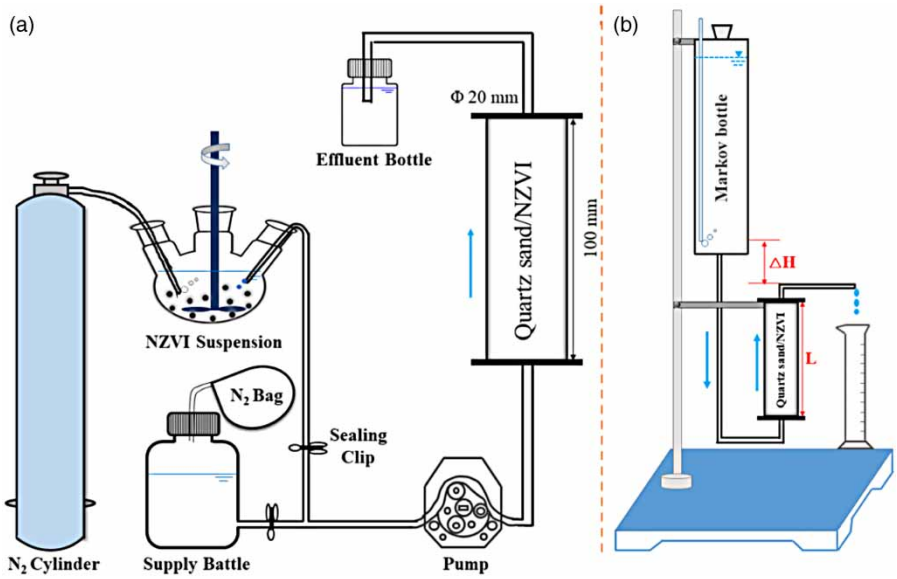

Figure 1 | The schematic of column setup.

the glue, and was used to measure the pore size of porous media. First, the solidified quartz sand was characterized by scanning electron microscopy (SEM) (SU8020, Japan), and then the images were analyzed with Nano-measure software to obtain the pore size distribution (Li *et al.* 2013).

(2) Saturated columns and tracer tests

After loading completely, each column was placed vertically and flushed with 60 mL 99.99% CO_2 with a peristaltic pump (BT100-1F, China). After CO_2 flushing, the column was saturated with 3 mM pH = 8.3 $NaHCO_3$ (background electrolyte solution) at a rate of 2.75 m/d, and then the saturated volume was recorded and defined as pore volume (PV). Subsequently, nonreactive tracer tests were conducted with 10 mM Br^- (prepared with a background electrolyte solution) at a rate of 2.75 m/d. Breakthrough data of tracer tests were analyzed by inverse function method to obtain the dispersion coefficient and assess whether there was a priority flow in the column, as shown in Supplementary Material, Figure S4 and Table 2. Dispersivity of saturated sand columns was greater than 19.28 cm, which indicated that there was not a priority flow (Koestel *et al.* 2013).

(3) Evaluation of constant head device

It has been reported that NZVI concentration used in the actual injection process was generally 1–20 g/L and injection velocity was usually 0.24–172 m/d (Mueller *et al.* 2012; Hosseini & Tosco 2013; Strutz *et al.* 2016a). In this study, 4 g/L NZVI suspension was injected into different sand columns at a flow velocity of 92 m/d. Obviously, saturated sand columns could be washed with high flow velocity. However, after flushing saturated sand columns at different flow velocities, how the constant head device (in Figure 1(b)) to determine the permeability of the sand column had changed was investigated.

Saturated sand columns were firstly flushed for 60 min at a rate of 2.75 m/d, and the volume of effluent was measured using the constant head device every 10 min (total measuring time was 120 min). At this time, q was defined as the outflow per unit time. Subsequently, saturated sand columns were washed at a rate of 138 m/d and 92 m/d respectively, and both were tested with the constant head device. In this process, I values of coarse sand, medium sand and fine sand columns were 0.4, 0.8 and 1.0, respectively. Additionally, in order to verify whether the constant head device could use Darcy's law to calculate hydraulic conductivity of saturated column, when I values of the constant head device were 0.2, 0.4, 0.6, 0.8 and 1.0, respectively, the volume of effluent was measure every 10 min (total measuring time was 60 min) to obtain overflow velocity V'.

(4) NZVI injection and permeability loss

NZVI suspension was dispersed using an electric mixer (IKA, Germany) at anaerobic atmosphere before use, and was continuously stirred during the injection process to minimize aggregation and sedimentation before injection into the column (Strutz *et al.* 2016a). A volume of 150 mL NZVI suspension was injected at a rate of 92 m/d, and then 200 mL background electrolyte solution was injected at the same velocity to flush the pipe. The hydraulic conductivity of saturated sand column

Table 2 | Basic parameters of experimental sand column

Media type	Units	Coarse sand	Medium sand	Fine sand
Filling mass	G	47.84	46.12	45.76
Pore value	mL	11.90	12.20	12.67
Porosity		0.38	0.39	0.40
Bulk density	g/cm^3	2.45	2.40	2.44
Dispersion coefficient	cm^2/d	8.60	6.23	4.36
Dispersivity	cm	0.012	0.009	0.007
NZVI concentration	g/L	4		
Injection velocity	m/d	92		
Injection volume	mL	150		
Flush volume	mL	200		

was measured by constant head device before and after NZVI injection. Permeability loss of saturated sand column was calculated by the following:

$$\text{Permeability loss} = 1 - \frac{K}{K_0} \tag{2}$$

where K and K_0 are hydraulic conductivity of saturated sand column, before and after NZVI injection.

2.4. Sample collection and measurement

In the process of Br^- penetration, every 0.15 mL sample of the effluent was collected by autosampler (Jiapeng SBS-100, China). The Br^- concentration was measured by ion chromatography (Metrohm 883, Switzerland). During NZVI the injection and flushing process, two effluents were collected separately, and then 2.5 mL concentrated HCl was added to dissolve the eluted NZVI. After the whole experimental column running, the solid samples in the column were individually taken out at a height of 1 cm, and then deposited NZVI was analyzed after freeze drying and acid digest. Fe concentration of solution was determined using inductively coupled plasma-optical emission spectrometry (Spectro, Germany).

3. RESULTS AND DISCUSSION

3.1. Evaluation of constant head device

After flushing saturated sand columns at different flow velocity, the relationship between q determined by evaluation of constant head device and time is shown in Figure 2(a). The q values of coarse sand and medium sand columns were observed to gradually increase with time, while that of fine sand column decreased after flushing at a rate of 2.75 m/d, which indicated that the overflow volume of saturated sand columns measured by the constant head device could not be stable for a long time under these conditions. However, all saturated sand columns had been washed at a rate of 138 m/d, then q of coarse sand, medium sand and fine sand columns did not change over time, and were 2.87, 30.5 and 17.1 mL/min, respectively. This might be because porous media particles could be arranged and distributed more uniformly and densely in a relatively short time under the action of larger hydrodynamic forces. Subsequently, after flushing saturated sand columns at a rate of 92 m/d, all q were almost the same as that at a rate of 138 m/d, and the error range was not more than 2.1%. As a result, when NZVI was injected into the saturated sand columns at a rate of 92 m/d, this velocity would not affect the hydraulic conductivity determined by the constant head device.

The results measured by the constant head device were used to calculate the hydraulic conductivity through the Darcy equation, in which method was evaluation, as shown in Figure 2(b). It could be seen that V' of saturated sand columns increased with an increase of I, and followed the trend of coarse sand > medium sand > fine sand. In addition, V' and I

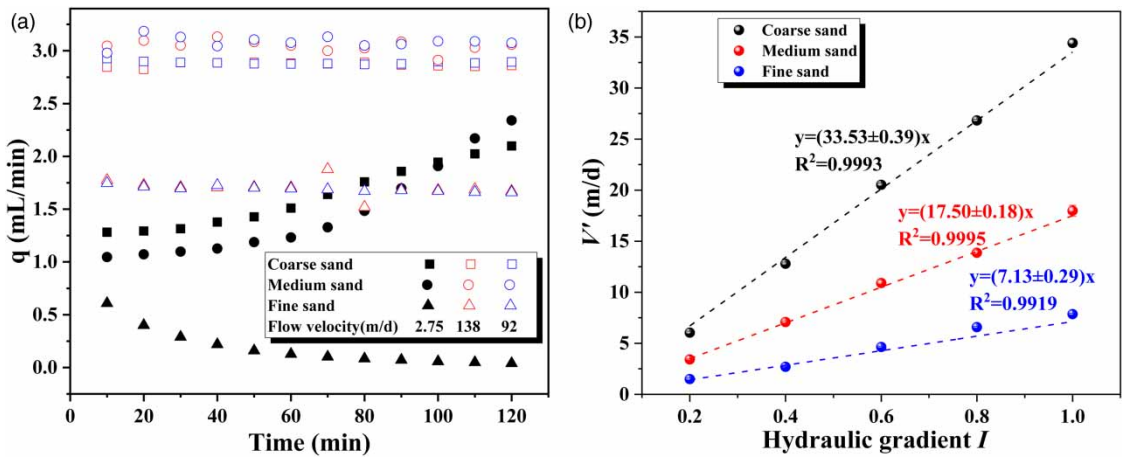

Figure 2 | (a) The change of overflow flow over time after flushing saturated sand columns at different flow velocities. (b) The relationship between overflow velocity and hydraulic gradient for different saturated sand columns (the dashed line represents the linear fit).

could be linearly fitted well (correlation coefficient $R^2 > 0.99$), and followed the form of $y = kx$ (k was constant), which was consistent with the Darcy equation. Therefore, it was feasible to determine the hydraulic conductivity of the saturated sand column using the constant head device. The hydraulic conductivities of coarse sand, medium sand and fine sand columns were 33.53, 17.50 and 7.13 m/d, respectively, which were within that of experienced value range (Ambraseys 1968).

3.2. Permeability loss and NZVI deposition

Figure 3 shows the permeability loss of different saturated sand columns after NZVI was injected. The permeability losses followed the trend of fine sand > medium sand > coarse sand, and were 91.93, 44.80 and 35.30%, respectively. However, after the saturated sand columns were washed at a rate of 138 m/d, the injection velocity of NZVI was 92 m/d, which had no effect on the permeability of saturated sand column determined by the constant head device (Figure 2(a)). Obviously, the NZVI injection transported in the column, and deposited, which resulted in reduced pore channels as well as permeability loss of sand columns.

As seen in Figure 4(a), after the injection process, the amounts of NZVI in the effluent in coarse sand, medium sand and fine sand columns were 4.63 mg, 0.11 mg and not detected, respectively. However, only 2.20 mg NZVI was detached in the column of coarse sand during the flushing process. Overall, the larger was the pore size of the porous media, the easier the nZVI was to transport (Saberinasr *et al.* 2016; Strutz *et al.* 2016b). Furthermore, eluted NZVI was less than 2‰ of the total injection amount at the inlet, indicating that transport ability of bare NZVI is relatively weak, which is consistent with results from a previous study (Tiraferri & Sethi 2009; Phenrat *et al.* 2010).

Under the same conditions, deposited $NZVI_{tot}$ amounts in coarse sand, medium sand and fine sand columns were 22.88, 26.38 and 14.08 g/kg, respectively (Figure 4(b)). Obviously, the NZVI content of coarse sand was lower than that of medium sand due to differences in NZVI elution during injection and flushing processes (Figure 4(a)). Although deposited $NZVI_{tot}$ in fine sand was the lowest, the permeability loss was the largest, which indicated that deposited $NZVI_{tot}$ in the different sand columns could not completely determine the loss of permeability. In addition, the spatial distribution of NZVI in different sand columns is shown in Figure 4(b). The amount of NZVI deposition was observed to gradually decrease along the column length, which was found for every column. Highest deposited nZVI localized at a distance of 1 cm from the inlet and followed the trend of fine sand > medium sand > coarse sand, and the proportions of deposited $NZVI_{tot}$ were 96.40, 38.81 and 25.43%, respectively. This is because the fine sand has a larger SSA and more attachment sites, which makes NZVI deposit faster (Raychoudhury *et al.* 2014; Li *et al.* 2016). When the distance from the inlet was greater than 3 cm, the amount of NZVI deposited in the coarse sand column was higher than in the other sand columns, which suggested that the distribution of NZVI injected in the coarse sand column was relatively uniform. Therefore, the distribution of NZVI deposited in the sand columns could affect the permeability loss.

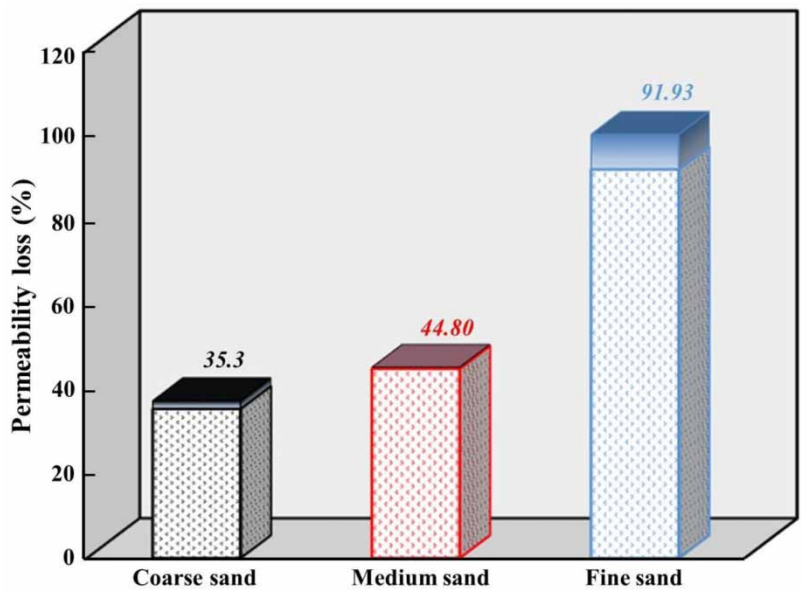

Figure 3 | The permeability loss of different saturated sand columns after NZVI injection (the gradient color filled box indicates the error bar).

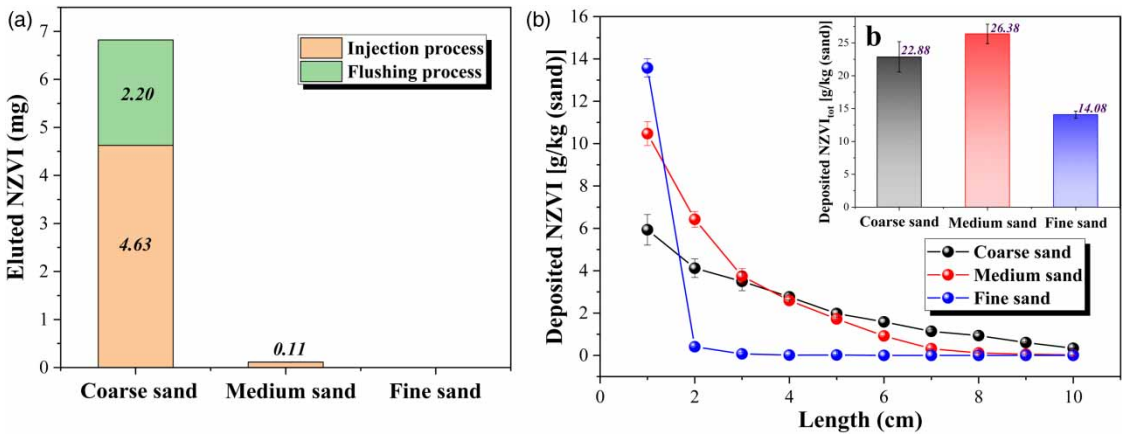

Figure 4 | (a) The content of eluted NZVI during the injection process and the flushing process for different sand columns. (b) Retention profiles along the column length of NZVI and deposited $NZVI_{tot}$ in different sand columns.

Simultaneously, the cumulative percentage of deposited NZVI (*CP*) in the different sand columns was analyzed, and calculated as follows:

$$CP = \frac{M_x}{M_r + M_e} \times 100\% \tag{3}$$

where *CP* is the cumulative percentage of deposited NZVI localized at a distance of x cm from the inlet, %; M_x is the total content of deposited NZVI localized at a distance of x cm from the inlet, mg; M_r is the total content of deposited NZVI in the sand column, mg; and M_e is the amount of eluted NZVI, mg.

It is shown in Figure 5(a) that the change of CP over transport distance was well in line with the index trend ($R^2 > 0.98$ and sum of squared residuals were relatively small), and fitted parameters are presented in Table 3. According to the colloid filtration theory, the distance at which 99% of nanoparticles are deposited in the porous media is defined as the maximum migration distance (He *et al.* 2009). Therefore, the maximum migration distances in the coarse sand, medium sand and fine sand columns were 16.78, 8.53 and 1.80 cm, respectively, which was similar to previous reports (Li *et al.* 2015).

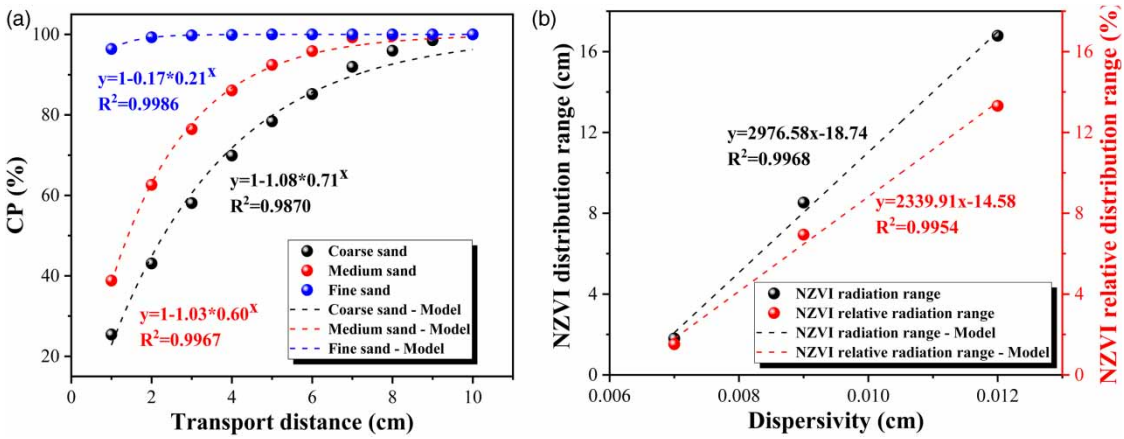

Figure 5 | (a) Cumulative percentage of deposited NZVI in the different sand columns. (b) The relationships between the dispersivity of porous media and the (relative) distribution range of NZVI.

Table 3 | Fitting parameter of cumulative percentage of deposited NZVI in the different sand columns

Parameter	Equation $y = 1 - B*A^x$				Maximum transport distance (cm)
	A	B	R^2	RSS	
Coarse sand	0.76	1.00	0.9992	1.51E-2	16.78
Medium sand	0.58	1.04	0.9986	6.99E-2	8.53
Fine sand	0.20	0.18	0.9991	1.21E-4	1.80

Note: A is between 0 and 1, and controls the uniformity of the distribution of NZVI in the sand column; B is affected by A, and both determine the transport distance of NZVI in the sand column.

Based on NZVI injection volume and PV of porous media, the migration distance of inert substance (such Cl^- and Br^-) and NZVI relative distribution range were calculated by the following:

$$L_{IS} = \frac{V_{NZVI} \times L}{V_{PV}} \tag{4}$$

$$\mathrm{RDR} = \frac{L_{NZVI}}{L_{IS}} \times 100\% \tag{5}$$

where L_{IS} is the migration distance of inert substance, cm; V_{NZVI} is NZVI injection volume, mL; V_{PV} is PV of porous media, mL; L is the length of the sand column, cm; RDR is NZVI relative distribution range, %; L_{NZVI} is NZVI distribution range, this is the maximum migration distance of NZVI, cm.

The relationships between the dispersivity of porous media and the (relative) distribution range of NZVI are as shown in Figure 5. The dispersivity of porous media has a good positive linear correlation with NZVI distribution range and NZVI relative distribution range ($R^2 > 0.99$). Under the conditions of this experiment, NZVI relative distribution ranges in the coarse sand, medium sand and fine sand columns were 13.31, 6.94 and 1.52%, respectively. These results indicate that the NZVI distribution range can be determined by the dispersivity of the aquifer.

3.3. Mechanism of permeability loss

The permeability loss was caused by the amount and distribution of NZVI deposited in the sand column, based on the above discussion. It was reported that clogging type could be classified into three types: surface clogging, inner clogging and mix clogging (including surface and inner clogging) (Du *et al.* 2014). When calculated according to Figure 4(b) and Table 4, the clogging types of NZVI in the coarse sand and medium sand columns were also mix clogging, while that in the fine sand column was surface clogging. These results are presented in Table 5. Therefore, the clogging mechanism of NZVI deposited in the fine sand column was surface filtration, while that in the coarse sand and medium sand columns included surface filtration and inner clogging.

It was found that colloid particle clogging in porous media highly depended on the colloid size and porous media properties (Bradford *et al.* 2002). The particle–particle and particle–collector contact were enhanced with a reduction in pore size of porous media (Saberinasr *et al.* 2016). Furthermore, the SSA of porous media was improved with a decrease in grain

Table 4 | Judgment criteria for clogging type of NZVI in the sand column

Clogging type	M_0/M_1	M_i/M_t
Surface clogging	>1	<0.5
Inner clogging	<1	>0.5
Mix clogging	≥1	>0.5

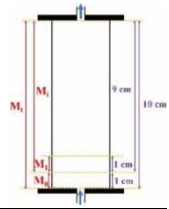

Note: M_0 is the amount of NZVI deposited at a distance of 1 cm from the inlet to the sand column; M_1 is the amount of NZVI deposited at a distance of 1–2 cm in the sand column; M_i is the amount of NZVI deposited at a distance from 1 cm to outlet in the sand column; M_t is the total amount of NZVI deposited in the sand column.

Table 5 | The clogging type and phenomenon of NZVI in the different sand columns

Porous media	Coarse sand	Medium sand	Fine sand
M_0/M_1	1.44	1.63	33.23
M_i/M_t	0.74	0.60	0.036
Clogging type	Mix clogging	Mix clogging	Surface clogging
Clogging phenomenon			

size, which provided more available attachment sites for particles (Raychoudhury *et al.* 2014; Li *et al.* 2016). Supplementary Material, Figure S4 shows that the average pore sizes of coarse sand, medium sand and fine sand were 55.28, 36.21 and 20.28 μm, respectively, and that of SSA were 74.9, 93.1 and 110.9 m^2/kg, respectively, as in Table 1. Therefore, NZVI injected into fine sand was deposited more quickly than into coarser sand, so that NZVI could be too late to migrate from the injection port, which would result in surface clogging and rapid decrease in permeability. Although surface clogging in coarse sand or medium sand also occurred with an increase in NZVI deposited in the injection port, the degree of surface clogging was relatively less serious than that of fine sand. In addition, the pore channels of coarse sand and medium sand gradually reduced when NZVI entered the porous media, especially for small pore channels occupied by NZVI deposition, which could hinder NZVI transport and cause inner clogging. The detail clogging mode of NZVI in porous media is depicted in Figure 6.

3.4. Application of NZVI injected in the field

NZVI injection can cause clogging and reduce permeability of an aquifer, which is conducive to the treatment of contaminant source zones due to a decrease in contaminant release, increase in reaction time of NZVI with pollutants and reduction in NZVI consumption or passivation by non-target pollutants, such as H_2O and nitrate. When clogging occurs, the rapid

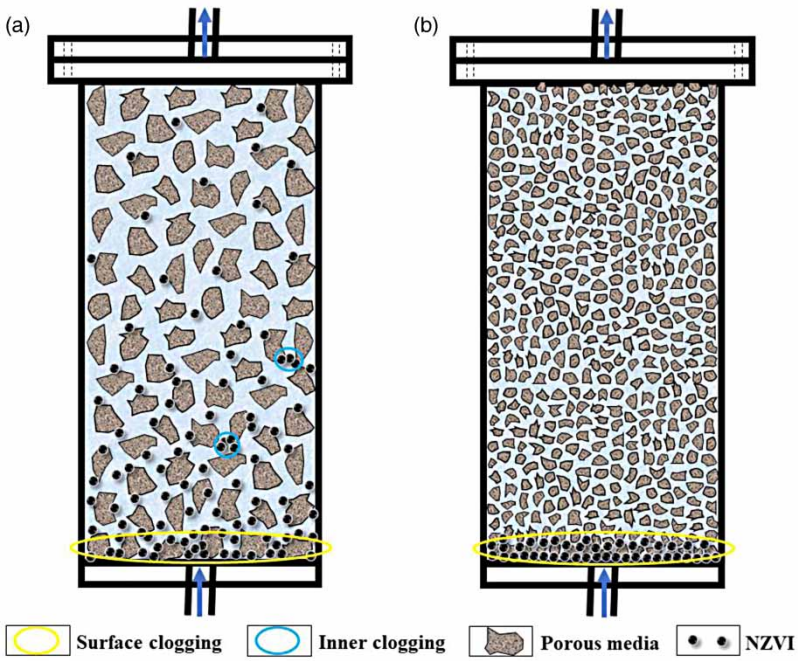

Figure 6 | The detail clogging mode of NZVI in porous media. (a) Coarse and medium sand; (b) fine sand.

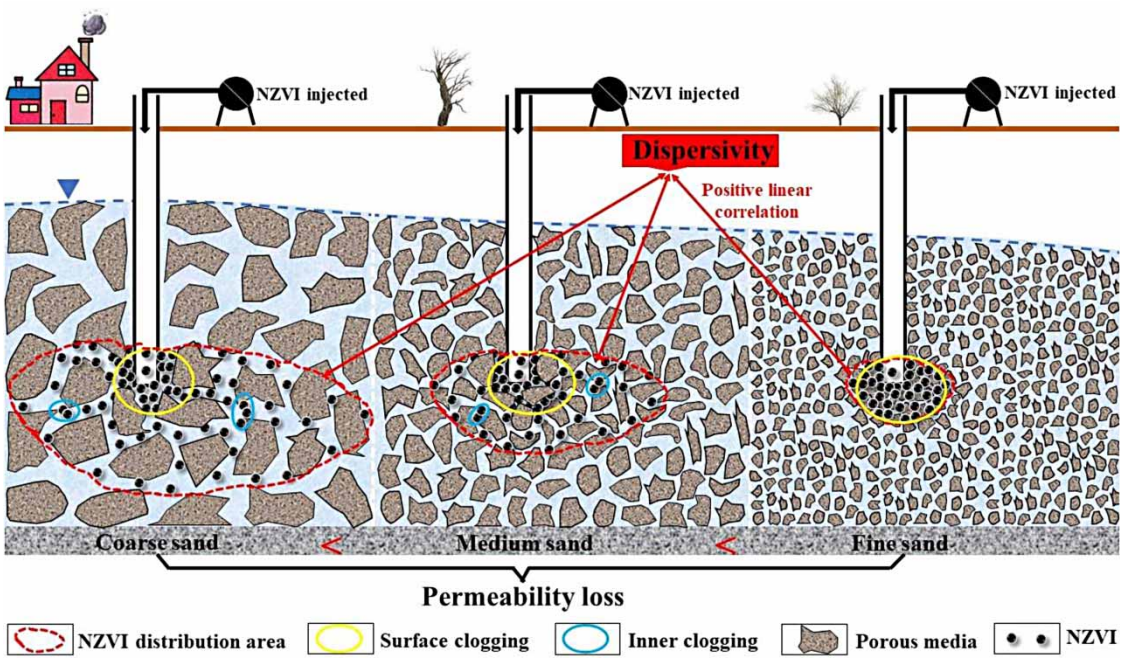

Figure 7 | The clogging model of NZVI injected in the field.

reduction in permeability would result in pressure at the injection point, which could hinder the further injection of NZVI and induce hydraulic fracturing. Figure 7 shows the clogging model of NZVI injected in the field. The permeability loss of NZVI injected into coarse sand, medium sand and fine sand aquifers increased sequentially. The NZVI distribution area in the aquifer was reduced with a decrease in grain size of the porous media, and showed a good positive linear correlation with the dispersivity of the porous media. In other words, the NZVI distribution area can be determined by NZVI injection volume and the dispersivity of the aquifer that is obtained by field tracer experiments. Furthermore, the clogging types for NZVI injected into coarse sand, medium sand and fine sand aquifers are mix clogging, mix clogging and surface clogging, respectively. Although surface clogging occurs in all aquifers, the amount of NZVI deposition and the rapid reduction in permeability at the injection point of the fine sand aquifer are larger than for coarser sand, which is more likely to cause hydraulic fracturing and then expand the area of the contaminant source zone. Therefore, the media type of contaminated aquifer should be considered using NZVI for in-situ remediation of the contaminant source zone.

4. CONCLUSIONS

In this work, the effect of NZVI injection on the permeability of different saturated porous media was investigated using the column tests. Before NZVI injection, the hydraulic conductivities of coarse sand, medium sand and fine sand columns determined by the constant head device were 33.53, 17.50 and 7.13 m/d, respectively. After NZVI injection, the permeability losses of porous media increased with a decrease in grain size, and that of coarse sand, medium sand and fine sand columns were 35.30, 44.80, and 91.93%, respectively. The amount and distribution of NZVI deposition jointly controlled the permeability loss of porous media. NZVI distribution area and the dispersivity of porous media were well in line with the positive linear correlation. Additionally, the mechanisms for permeability loss for coarse sand and medium sand columns were inner clogging besides surface filtration for fine sand column. Although surface clogging occurred in all sand columns, the proportion deposited at a distance of 1 cm from the inlet of the fine sand column was 96.40%, which was much larger than that of the coarse sand and medium sand columns (25.43 and 38.81%, respectively). It was clear that the permeability of the fine sand columns declined faster, so that NZVI would be more difficult to inject. Therefore, these results may provide significant information for NZVI field injection and successful groundwater remediation, especially considering the media type of the contaminated aquifer to avoid hydraulic fracturing and expansion of the area of contaminant source zone.

ACKNOWLEDGEMENTS

This study was supported by the Research Fund of China Geological Survey (DD20190323) and Natural Science Foundation of China (No. 41572229).

DATA AVAILABILITY STATEMENT

All relevant data are included in the paper or its Supplementary Information.

REFERENCES

Ambraseys, N. 1968 *Rock Mechanics in Engineering Practice*. London UK: John Wiley & Sons.

Babakhani, P., Fagerlund, F., Shamsai, A., Lowry, G. V. & Phenrat, T. 2018 Modified modflow-based model for simulating the agglomeration and transport of polymer-modified Fe(0) nanoparticles in saturated porous media. *Environmental Science and Pollution Research International* **25**, 7180–7199.

Bradford, S. A., Yates, S. R., Bettahar, M. & Simunek, J. 2002 Physical factors affecting the transport and fate of colloids in saturated porous media. *Water Resources Research* **38** (12), 63-1–63-12.

Comba, S., Molfetta, A. D. & Sethi, R. 2011 A comparison between field applications of nano-, micro-, and millimetric zero-valent iron for the remediation of contaminated aquifers. *Water Air and Soil Pollution* **215** (1–4), 595–607.

Dong, H. & Lo, I. M. 2013 Influence of calcium ions on the colloidal stability of surface-modified nano zero-valent iron in the absence or presence of humic acid. *Water Research* **47** (7), 2489–2496.

Du, X., Fang, Y., Wang, Z., Hou, J. & Ye, X. 2014 The prediction methods for potential suspended solids clogging types during managed aquifer recharge. *Water* **6** (4), 961–975.

Fu, F., Dionysiou, D. D. & Liu, H. 2014 The use of zero-valent iron for groundwater remediation and wastewater treatment: a review. *Journal of Hazardous Materials* **267**, 194–205.

Guan, X. H., Sun, Y. K., Qin, H. J., Li, J. X., Lo, I. M. C., He, D. & Dong, H. R. 2015 The limitations of applying zero-valent iron technology in contaminants sequestration and the corresponding countermeasures: the development in zero-valent iron technology in the last two decades (1994–2014). *Water Research* **75**, 224–248.

Harendra, S. & Vipulanandan, C. 2011 Fe/Ni bimetallic particles transport in columns packed with sandy clay soil. *Industrial & Engineering Chemistry Research* **50** (1), 404–411.

He, F., Zhang, M., Qian, T. & Zhao, D. 2009 Transport of carboxymethyl cellulose stabilized iron nanoparticles in porous media: column experiments and modeling. *Journal of Colloid and Interface Science* **334** (1), 96–102.

He, Y., Lin, H., Dong, Y., Li, B., Wang, L., Chu, S., Luo, M. & Liu, J. 2018 Zeolite supported Fe/Ni bimetallic nanoparticles for simultaneous removal of nitrate and phosphate: synergistic effect and mechanism. *Chemical Engineering Journal* **347**, 669–681.

Hosseini, S. M. & Tosco, T. 2013 Transport and retention of high concentrated nano-Fe/Cu particles through highly flow-rated packed sand column. *Water Research* **47** (1), 326–338.

Jung, B., O'Carroll, D. & Sleep, B. 2014 The influence of humic acid and clay content on the transport of polymer-coated iron nanoparticles through sand. *The Science of the Total Environment* **496**, 155–164.

Karn, B., Kuiken, T. & Otto, M. 2009 Nanotechnology and in situ remediation: a review of the benefits and potential risks. *Environmental Health Perspectives* **117** (12), 1813–1831.

Koestel, J. K., Norgaard, T., Luong, N. M., Vendelboe, A. L., Moldrup, P., Jarvis, N. J., Lamande, M., Iversen, B. V. & Jonge, L. W. 2013 Links between soil properties and steady-state solute transport through cultivated topsoil at the field scale. *Water Resources Research* **49** (2), 790–807.

Li, M., Hu, M., Liu, Q., Ma, S. & Sun, P. 2013 Microstructure characterization and NO_2-sensing properties of porous silicon with intermediate pore size. *Applied Surface Science* **268**, 188–194.

Li, H., Zhao, Y. S., Han, Z. T. & Hong, M. 2015 Transport of sucrose-modified nanoscale zero-valent iron in saturated porous media: role of media size, injection rate and input concentration. *Water Science and Technology : A Journal of the International Association on Water Pollution Research* **72** (9), 1463–1471.

Li, J., Rajajayavel, S. R. C. & Ghoshal, S. 2016 Transport of carboxymethyl cellulose-coated zerovalent iron nanoparticles in a sand tank: effects of sand grain size, nanoparticle concentration and injection velocity. *Chemosphere* **150**, 8–16.

Litton, G. M. & Olson, T. M. 1993 Colloid deposition rates on silica bed media and artifacts related to collector surface preparation methods. *Environmental Science & Technology* **27** (1), 185–193.

Micic, V., Bossa, N., Schmid, D., Wiesner, M. R. & Hofmann, T. 2020 Groundwater chemistry has a greater influence on the mobility of nanoparticles used for remediation than the chemical heterogeneity of aquifer media. *Environmental Science & Technology* **54** (2), 1250–1257.

Mondal, A., Dubey, B. K., Arora, M. & Mumford, K. 2021 Porous media transport of iron nanoparticles for site remediation application: a review of lab scale column study, transport modelling and field-scale application. *Journal of Hazardous Materials* **403**, 123443.

Mueller, N. C., Braun, J., Bruns, J., Cernik, M., Rissing, P., Rickerby, D. & Nowack, B. 2012 Application of nanoscale zero valent iron (NZVI) for groundwater remediation in Europe. *Environmental Science and Pollution Research International* **19** (2), 550–558.

Mystrioti, C., Papassiopi, N., Xenidis, A., Dermatas, D. & Chrysochoou, M. 2015 Column study for the evaluation of the transport properties of polyphenol-coated nanoiron. *Journal of Hazardous Materials* **281**, 64–69.

Mystrioti, C., Ntrouka, A., Thymi, S., Papassiopi, N. & Xenidis, A. 2020 Effect of limestone grain size on the mobility of green nanoiron suspension. *Applied Geochemistry* **122**, 204759.

Noubactep, C., Care, S. & Crane, R. 2012 Nanoscale metallic iron for environmental remediation: prospects and limitations. *Water Air and Soil Pollution* **223** (3), 1363–1382.

Ostad-Ali-Askari, K. & Shayannejad, M. 2021 Quantity and quality modelling of groundwater to manage water resources in Isfahan-Borkhar Aquifer. *Environment, Development and Sustainability* **23** (11), 15943–15959.

Phenrat, T., Liu, Y., Tilton, R. D. & Lowry, G. V. 2009a Adsorbed polyelectrolyte coatings decrease Fe-0 nanoparticle reactivity with TCE in water: conceptual model and mechanisms. *Environmental Science & Technology* **43** (5), 1507–1514.

Phenrat, T., Kim, H. J., Fagerlund, F., Illangasekare, T., Tilton, R. D. & Lowry, G. V. 2009b Particle size distribution, concentration, and magnetic attraction affect transport of polymer-modified Fe^0 nanoparticles in sand columns. *Environmental Science & Technology* **43** (13), 5079–5085.

Phenrat, T., Cihan, A., Kim, H. J., Mital, M., Illangasekare, T. & Lowry, G. V. 2010 Transport and deposition of polymer-modified Fe^0 nanoparticles in 2-D heterogeneous porous media: effects of particle concentration, Fe^0 content and coatings. *Environmental Science & Technology* **44** (23), 9086–9093.

Raychoudhury, T., Naja, G. & Ghoshal, S. 2010 Assessment of transport of two polyelectrolyte-stabilized zero-valent iron nanoparticles in porous media. *Journal of Contaminant Hydrology* **118** (3–4), 143–151.

Raychoudhury, T., Tufenkji, N. & Ghoshal, S. 2014 Straining of polyelectrolyte-stabilized nanoscale zero valent iron particles during transport through granular porous media. *Water Research* **50**, 80–89.

Saberinasr, A., Rezaei, M., Nakhaei, M. & Hosseini, S. M. 2016 Transport of CMC-stabilized nZVI in saturated sand column: the effect of particle concentration and soil grain size. *Water, Air, & Soil Pollution* **227** (10), 394.

Saleh, N., Kim, H. J., Phenrat, T., Matyjaszewski, K., Tilton, R. D. & Lowry, G. V. 2008 Ionic strength and composition affect the mobility of surface-modified Fe^0 nanoparticles in water-saturated sand columns. *Environmental Science & Technology* **42** (9), 3349–3355.

Strutz, T. J., Hornbruch, G., Dahmke, A. & Kober, R. 2016a Effect of injection velocity and particle concentration on transport of nanoscale zero-valent iron and hydraulic conductivity in saturated porous media. *Journal of Contaminant Hydrology* **191**, 54–65.

Strutz, T. J., Hornbruch, G., Dahmke, A. & Kober, R. 2016b Influence of permeability on nanoscale zero-valent iron particle transport in saturated homogeneous and heterogeneous porous media. *Environmental Science and Pollution Research International* **23** (17), 17200–17209.

Tian, Y., Gao, B., Silvera-Batista, C. & Ziegler, K. J. 2010 Transport of engineered nanoparticles in saturated porous media. *Journal of Nanoparticle Research* **12** (7), 2371–2380.

Tiraferri, A. & Sethi, R. 2009 Enhanced transport of zerovalent iron nanoparticles in saturated porous media by guar gum. *Journal of Nanoparticle Research* **11** (3), 635–645.

Tosco, T. & Sethi, R. 2010 Transport of non-Newtonian suspensions of highly concentrated micro- and nanoscale iron particles in porous media: a modeling approach. *Environmental Science & Technology* **44** (23), 9062–9068.

Tosco, T., Petrangeli Papini, M., Cruz Viggi, C. & Sethi, R. 2014 Nanoscale zerovalent iron particles for groundwater remediation: a review. *Journal of Cleaner Production* **77**, 10–21.

Wei, Y. T., Wu, S. C., Chou, C. M., Che, C. H., Tsai, S. M. & Lien, H. L. 2010 Influence of nanoscale zero-valent iron on geochemical properties of groundwater and vinyl chloride degradation: a field case study. *Water Research* **44** (1), 131–140.

Wu, C., Tu, J., Liu, W., Zhang, J., Chu, S., Lu, G., Lin, Z. & Dang, Z. 2017 The double influence mechanism of pH on arsenic removal by nano zero valent iron: electrostatic interactions and the corrosion of Fe^0. *Environmental Science: Nano* **4** (7), 1544–1552.

Yang, X., Zhang, C., Liu, F., Tang, J., Huang, F. & Zhang, L. 2019 Diversity in the species and fate of chlorine during TCE reduction by two nZVI with non-identical anaerobic corrosion mechanism. *Chemosphere* **230**, 230–238.

Yang, X., Zhang, C., Liu, F. & Tang, J. 2021 Groundwater geochemical constituents controlling the reductive dechlorination of TCE by nZVI: evidence from diverse anaerobic corrosion mechanisms of nZVI. *Chemosphere* **262**, 127707.

Zheng, T., Zhan, J., He, J., Day, C., Lu, Y., McPherson, G. L., Piringer, G. & John, V. T. 2008 Reactivity characteristics of nanoscale zerovalent iron-silica composites for trichloroethylene remediation. *Environmental Science & Technology* **42** (12), 4494–4499.

Zou, Y. D., Wang, X. X., Khan, A., Wang, P. Y., Liu, Y. H., Alsaedi, A., Hayat, T. & Wang, X. K. 2016 Environmental remediation and application of nanoscale zero-valent iron and its composites for the removal of heavy metal ions: a review. *Environmental Science & Technology* **50** (14), 7290–7304.

First received 13 August 2021; accepted in revised form 29 October 2021. Available online 9 November 2021